ISSN 1070-3284, Russian Journal of Coordination Chemistry, 2024, Vol. 50, No. 7, pp. 476–484. © Pleiades Publishing, Ltd., 2024.

Crystal Structure of Lanthanide Salts with 2,4-Dichlorophenoxyacetic Acid

M. A. Kiskin[a], O. V. Konnik[b], V. F. Shul'gin[b, *], and A. N. Gusev[b]

[a] *Kurnakov Institute of General and Inorganic Chemistry, Russian Academy of Sciences, Moscow, Russia*

[b] *Vernadsky Crimea Federal University, Simferopol, Crimea, Russia*

**e-mail: shuvic@gmail.com*

Received February 27, 2024; revised April 9, 2024; accepted April 24, 2024

Abstract—Compounds of three types, $[LnL_3(C_2H_5OH)]$ (Ln = Nd (**I**), Sm (**II**), Eu (**III**)), $[LnL_3(H_2O)]$ (Ln = Gd (**IV**), Tb (**V**)), and $[DyL_2(NO_3)(C_2H_5OH)_2]$ (**VI**), were obtained by reactions of lanthanide nitrate with NaL (L^- = 2,4-dichlorophenoxyacetate anion) in ethanol. The composition and structure of complexes **I**–**VI** were investigated by elemental and thermogravimetric analysis, IR spectroscopy, and X-ray diffraction (nos. 2311578 (**I**), 2311579 (**II**), 2311580 (**III**), 2311581 (**IV**), 2311582 (**VI**)). All compounds have a one-dimensional polymer structure in which metal atoms are connected by bridging carboxylate groups. The π–π interactions and intermolecular contacts between the chains give rise to a three-dimensional supramolecular structure.

Keywords: carboxylates, 2,4-dichlorophenoxyacetic acid, lanthanides, noncovalent interactions, X-ray diffraction analysis

DOI: 10.1134/S107032842460030X

INTRODUCTION

Coordination compounds based on trivalent rare earth metal cations are of great interest, as they behave as molecular magnets [1] and exhibit narrow-band luminescence [2–5] and proton conductivity [6]. The lanthanide metal-organic frameworks are widely used in displays and lighting equipment [7–11], luminescent thermometers [12], and fluorescence sensors, in anti-counterfeiting and information storage [13–16]. The benefits manifested in these applications are environmental friendliness, energy saving, high efficiency, and long service life [17]. In the design of this type of materials, the attention is focused on the organic ligand, including not only its ability to form a cluster [18], but also the ability to form intercluster bonds. An example of such ligands is 2,4-dichlorophenoxyacetic acid (HL), which tends to form π–π-supramolecular interactions and a branched network of intermolecular contacts [19]. Analysis of the crystal structures of f-element 2,4-dichlorophenoxyacetates [20–24] and their ability to form stacking interactions resulted in identification of a few compounds that have this type of intermolecular contacts. In [23, 24], additional bipyridine ligands were introduced to fabricate supramolecular structures. In a systematic study of lanthanide 2,4-dichlorophenoxyacetates obtained from DMF, no stacking interactions involving aromatic systems were detected [25]. It is of interest to study the composition and structure of lanthanide 2,4-dichlorophenoxyacetate salts prepared in less polar solvents, first of all aqueous ethanol.

EXPERIMENTAL

Commercial reagent grade lanthanide nitrates, 2,4-dichlorophenoxyacetic acid (>99%), and ethanol (96%) were used as received.

Synthesis of lanthanide salts of 2,4-dichlorophenoxyacetic acid (general procedure). The compounds were obtained by the reaction of a specified lanthanide nitrate (0.35 mmol) dissolved in 96% aqueous ethanol (10 mL) with a solution of sodium 2,4-dichlorophenoxyacetate (1.05 mmol) in ethanol (40 mL). The resulting solution was magnetically stirred with heating to 70°C for 30 min and left to cool down until a crystalline solid formed. The crystals were collected on a filter, washed with a small amount of ethanol, and dried in air at room temperature. The product yield was approximately 60% based on the lanthanide salt.

$[NdL_3(C_2H_5OH)]$ (I). IR (ν, cm^{-1}): 3425, 1666, 1594, 1561, 1477, 1459, 1426, 1391, 1335, 1285, 1265, 1246, 1230, 1104, 1073, 1063, 1036, 940, 869, 838, 802, 769, 715, 698, 646, 603, 558, 466, 442, 407.

For $C_{26}H_{21}O_{10}Cl_6Nd$		
Anal. calcd., %	C, 36.72	H, 2.48
Found, %	C, 36.37	H, 1.97

$[SmL_3(C_2H_5OH)]$ (II). IR (ν, cm^{-1}): 3353, 1652, 1571, 1476, 1449, 1424, 1390, 1334, 1287, 1263, 1233, 1105, 1075, 1045, 937, 869, 839, 800, 767, 717, 696, 647, 605, 557, 468, 441.

For $C_{26}H_{21}O_{10}Cl_6Sm$

Anal. calcd., %	C, 36.46	H, 2.47
Found, %	C, 36.17	H, 2.71

$[EuL_3(C_2H_5OH)]$ (III). IR (ν, cm^{-1}): 3368, 1650, 1592, 1573, 1475, 1450, 1432, 1382, 1333, 1287, 1268, 1255, 1233, 1102, 1075, 1045, 937, 864, 839, 803, 715, 698, 663, 645, 603, 556, 462.

For $C_{26}H_{21}O_{10}Cl_6Eu$

Anal. calcd., %	C, 36.39	H, 2.47
Found, %	C, 36.30	H, 2.63

$[GdL_3(H_2O)]$ (IV). IR (ν, cm^{-1}): 3283, 1637, 1589, 1573, 1475, 1450, 1429, 1390, 1335, 1286, 1263, 1255, 1226, 1104, 1077, 1043, 926, 875, 838, 801, 716, 696, 647, 606, 556, 465, 439.

For $C_{24}H_{17}O_{10}Cl_6Gd$

Anal. calcd., %	C, 34.51	H, 2.05
Found, %	C, 34.21	H, 2.28

$[TbL_3(H_2O)]$ (V). IR (ν, cm^{-1}): 3293, 1650, 1584, 1554, 1475, 1451, 1430, 1417, 1391, 1334, 1286, 1264, 1252, 1227, 1154, 1104, 1078, 1044, 956, 942, 864, 838, 802, 766, 716, 647, 606, 556, 475, 440, 414.

For $C_{24}H_{17}O_{10}Cl_6Tb$

Anal. calcd., %	C, 34.44;	H, 2.05.
Found, %	C, 34.46;	H, 2.27.

$[DyL_2(NO_3)(C_2H_5OH)_2]$ (VI). IR (ν, cm^{-1}): 3407, 1650, 1585, 1577, 1554, 1507, 1479, 1454, 1434, 1398, 1338, 1286, 1273, 1253, 1225, 1161, 1123, 1107, 1074, 1034, 1027, 927, 878, 839, 805, 793, 768, 741, 713, 646, 593, 577, 558, 470, 450, 416.

For $C_{20}H_{22}NO_{11}Cl_4Dy$

Anal. calcd., %	C, 31.74	H, 2.93	N, 1.85
Found, %	C, 31.97	H, 2.67	N, 1.80

Elemental analysis was performed on a EURO-Vestor 3000A automatic analyzer. IR spectra were recorded on a Spectrum Two Fourier transform infrared spectrometer with an attenuated total internal reflection attachment (Perkin Elmer). Thermogravimetric studies were performed on an STA 6000 simultaneous thermal analyzer in a nitrogen atmosphere at a heating rate of 10°C/min.

X-ray diffraction study. The crystals suitable for X-ray diffraction were picked from the main bulk of the obtained product. The single crystal X-ray diffraction study was performed on Bruker Smart APEX II (for **I**–**III**, **V** and **VI**) and Bruker D8 Venture (for **IV**) diffractometers equipped by a CCD detector and a monochromatic radiation source (MoK_α, λ = 0.71073 Å, graphite monochromator) using standard procedures [26]. Semiempirical absorption correction was applied for all structures [27]. In structures **I**–**IV**, residual electron density was present in the local environment of lanthanide atoms, which can be caused by imperfection of absorption corrections and small size of needle-shaped crystals. The structures were solved by the direct methods and refined in the full-matrix anisotropic approximation for all non-hydrogen atoms. The calculations were carried out using the SHELX-2014/2015 [28] and Olex2 [29] programs. The RIGU (for the O(4)–C(9)–C(10)–O(5) moiety in **II**) and ISOR (for the O(8) atom in **II** and for the O(7) atom in **IV**) restraints were used in the structure solution. The hydrogen atoms were generated geometrically and refined in the riding model. The position of the H atom at the O atom of the ethanol molecule in **I**–**III** and **VI** was fixed by the AFIX 43 constraints; the H atom positions in the water molecule of **V** were fixed by AFIX 7. The geometry of metal atom polyhedra was determined using the SHAPE 2.1 program [30]. Crystallographic parameters and structure refinement details are given in Table 1.

The atom coordinates and thermal parameters and the list of all reflections were deposited with the Cambridge Crystallographic Data Centre (CCDC nos. 2311578 (**I**), 2311579 (**II**), 2311580 (**III**) 2311581 (**IV**), 2311582 (**VI**); deposit@ccdc.cam.ac.uk or http://www.ccdc.cam.ac.uk/structures).

The isostructural nature of compounds **V** and **IV** was determined by analysis of unit cell parameters for single crystal.

RESULTS AND DISCUSSION

The thermogravimetric curve for samples **I**–**III** in the temperature range from 90 to 140°C shows a 4–5% decrease in the mass accompanied by an endotherm in the DSC curve. This is in a reasonably good agreement with the loss of one ethanol molecule (theoretically, 5.4%). The compounds are stable up to 185°C. For complexes **IV** and **V**, the loss of 3% of mass takes place in the temperature range of 120–155°C, which corresponds to the loss of the inner-sphere water molecule. The elimination of ethanol molecule present in complex **VI** occurs in the temperature range of 30–80°C. At higher temperature, slow mass loss takes place, with no thermal stability range being present.

In the IR spectra of the studied carboxylates, the coordination of the acid anion to a lanthanide cation is accompanied by a low-frequency shift of the band

Table 1. Crystallographic parameters and structure refinement details for compounds **I**–**VI**

Parameter	Value				
	I	**II**	**III**	**IV**	**VI**
Molecular formula	$C_{26}H_{21}O_{10}Cl_6Nd$	$C_{26}H_{21}O_{10}Cl_6Sm$	$C_{26}H_{21}O_{10}Cl_6Eu$	$C_{24}H_{17}O_{10}Cl_6Gd$	$C_{20}H_{22}NO_{11}Cl_4Dy$
M	850.37	856.48	858.09	835.32	756.68
Crystal size, mm	0.1 × 0.01 × 0.01	0.12 × 0.01 × 0.01	0.4 × 0.05 × 0.05	0.25 × 0.08 × 0.02	0.3 × 0.01 × 0.01
T, K	150(2)	100(2)	100(2)	100	100
Space group; Z	$P\bar{1}$; 2	$P\bar{1}$; 2	$P\bar{1}$; 2	$P2_1/c$; 4	$C2/c$; 4
a, Å	7.8856(6)	7.8287(9)	7.8044(7)	10.0979(10)	25.871(2)
b, Å	12.8511(9)	12.7987(15)	12.8035(9)	35.341(2)	10.8251(10)
c, Å	15.3511(14)	15.3489(18)	15.3632(12)	7.9104(6)	9.3742(8)
α, deg	80.273(3)	80.250(4)	80.188(2)	90	90
β, deg	77.621(3)	77.618(3)	77.613(3)	96.800(2)	98.339(3)
γ, deg	87.484(3)	87.350(3)	87.271(2)	90	90
V, Å^3	1497.6(2)	1480.4(3)	1477.4(2)	2803.1(4)	2597.6(4)
ρ_{calcd}, g/cm^3	1.886	1.921	1.929	1.969	1.935
μ, mm^{-1}	2.324	2.581	2.722	2.978	3.347
Data collection range of θ, deg	1.94–26.73	2.29–28.28	2.29–28.28	2.03–33.14	2.91–30.51
Ranges hkl of reflection indices	$-9 \le h \le 9$, $-16 \le k \le 12$, $-19 \le l \le 16$	$-10 \le h \le 9$, $-17 \le k \le 17$, $-20 \le l \le 20$	$-10 \le h \le 10$, $-17 \le k \le 14$, $-20 \le l \le 19$	$-16 \le h \le 18$, $-53 \le k \le 50$, $-12 \le l \le 12$	$-27 \le h \le 34$, $-9 \le k \le 15$, $-11 \le l \le 13$
Number of measured/ unique reflections	9783/6116	12015/7237	13683/7264	32330/10031	6999/3803
Number of reflections with $I \ge 2\sigma(I)$	3986/389	5398/388	6616/389	8249/371	3335/171
R_{int}	0.0639	0.0610	0.0490	0.0590	0.0292
T_{min}/T_{max}	0.5438/0.7461	0.5391/0.7461	0.4506/0.7466	0.3914/0.7465	0.5278/0.7465
S	1.083	1.032	1.051	1.094	1.038
R_1, wR_2 ($I \ge 2\sigma(I)$)	0.0690, 0.0896	0.0692, 0.1074	0.0474, 0.1255	0.0542, 0.1129	0.0290, 0.0559
R_1, wR_2 (all vales)	0.1226, 0.1032	0.0996, 0.1177	0.0517, 0.1292	0.0717, 0.1198	0.0364, 0.0585
$\Delta\rho_{min}/\Delta\rho_{max}$, e/Å^3	−2.316/1.884	−3.358/3.035	−4.999/3.223	−5.798/2.650	−0.932/0.865

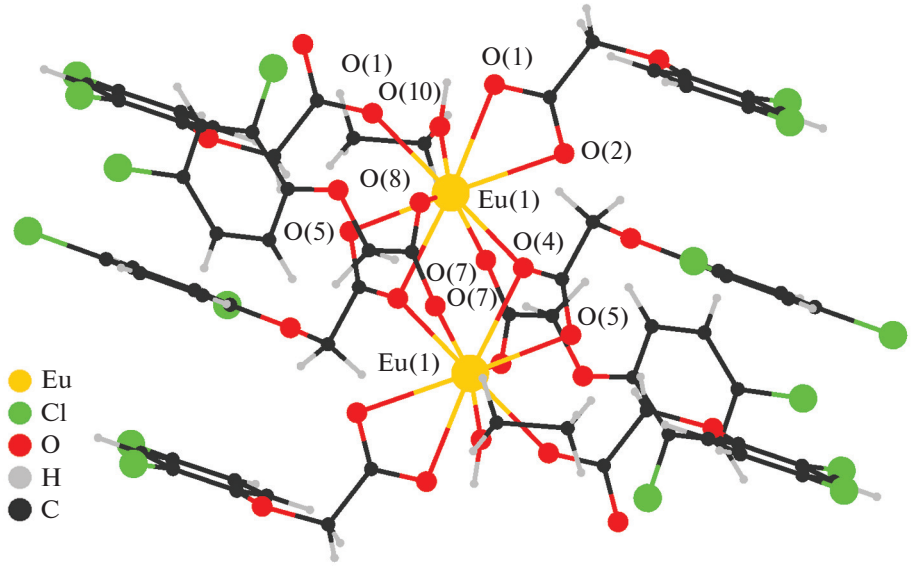

Fig. 1. Centrosymmetric dimeric fragment of the polymer chain in **III** (different coordination modes of the carboxylate anion are shown).

that could be assigned to the asymmetric stretching modes of the carboxylate anion (the range from 1594 to 1554 cm^{-1}). The symmetric vibrations of the carboxylate anion occur in the 1477–1418 cm^{-1} range. This is accompanied by splitting of each stretching mode into two bands. The frequency difference $\Delta\nu = \nu_{as} - \nu_{s} = 130–170$ cm^{-1} is typical of the chelating function of the carboxylate anion. The absorption bands for the asymmetric and rocking stretching vibrations of the Ar–O–C group are in the 1287–1225 cm^{-1} range. The series of bands in the 1107–1034 cm^{-1} frequency range can be assigned to the Ar–O–C stretching modes and the vibrational modes of the chlorine–carbon bonds in the benzene ring (strong band in the 1073–1078 cm^{-1} range). Numerous absorption bands in the 900–760 cm^{-1} range are characteristic of in-plane and out-of-plane bending vibrations of the carbon–hydrogen bonds of the benzene ring. The broad bands with absorption maxima in the 3425–3293 cm^{-1} were assigned to the stretching modes of the bound OH groups of ethanol and water molecules.

The IR spectrum of sample **VI** does not show a very strong absorption band in the 1400–1350 cm^{-1} range. Meanwhile, there are new bands, not inherent in other compounds, at 1507, 1273, 1027, and 793 cm^{-1}, which attest to the coordination of the nitrate anion to the metal cation [31].

X-ray diffraction studies of the obtained samples showed that all compounds were one-dimensional polymers, which can be divided into three structural groups. The first group includes isostructural metal-organic frameworks of neodymium, samarium, and europium. In each of them, one-dimensional polymer consists of $[Ln_2L_6(C_2H_5OH)_2]$ dimeric repeating units connected to one another (Fig. 1). The carboxylate ligands exhibit two coordination modes, bridging bidentate and chelating bridging tridentate modes. Thus, the coordination mode of one carboxylate anion differs from that in the neodymium aqua complex with 2,4-dichlorophenoxyacetate anion [21], in which it performs the bidentate function. The ethanol molecule completes the coordination number of the central atom to nine. The coordination polyhedron corresponds to a monocapped tetragonal antiprism. Selected bond lengths in the coordination polyhedron and distances between the central atoms in **I**–**VI** are given in Table 2. The decrease in the distance between metal cations is caused by the reduction of the ion radius in the lanthanide series.

In the gadolinium **IV** and terbium **V** metal-organic frameworks, the ninth site is occupied by a water molecule (Fig. 2). The tridentate chelating bridging function of two carboxylate anions is retained, while the third anion performs a bidentate function. The geometry of the coordination polymer corresponds to a monocapped tetragonal antiprism. Despite the decrease in the metal atom radii, the distance between the central atoms increases. This is attributable to the replacement of the bidentate bridging function by the bidentate function for the third ligand.

The dysprosium compound **VI** differs drastically in the composition from the above-described compounds. The coordination polyhedron of the central atom has a square antiprism geometry, with the coordination number of the central atom being eight (Fig. 3). Two carboxylate anions perform the bidentate

Table 2. Selected bond lengths and distances between the central atoms (Å) in **I**–**VI**

Bond	I	II	III	IV	VI
Ln–O(η,μ-O_2CR)	2.413(5)–2.578(5)	2.392(5)–2.539(5)	2.386(3)–2.526(3)	2.374(4)–2.487(4)	
Ln–O(η-O_2CR/η-O_2NO)				2.393(4), 2.464(4)	2.494(2)
Ln–O(μ-O_2CR)	2.393(4), 2.567(5)	2.357(5), 2.553(5)	2.347(3), 2.527(3)		2.254(2), 2.3490(18)
Ln–O(C_2H_5OH/H_2O)	2.481(5)/–	2.443(5)/–	2.433(3)/–	–/2.438(5)	2.3882(19)/–
Ln...Ln	4.0419(10), 4.1811(10)	4.0113(9), 4.1522(9)	3.9996(5), 4.1425(5)	4.064(4)	4.8905(6)

bridging function, and the nitrate anion is coordinated in the bidentate mode. The other two sites in the coordination polyhedron are occupied by ethanol molecules. All this results in increase in the distance between the dysprosium cations to 4.890 Å. The coordination polymer has a linear zigzag shape.

A distinctive feature of the crystal structure of the compounds is the presence of intrachain π...π interactions (stacking) in **I**–**III** and interchain π...π contacts in all compounds, resulting in the formation of a layered (for **I**–**IV**) or three-dimensional (for **VI**) supramolecular structure (Figs. 4–6). The stacking interaction parameters are given in Table 3. The crystal lattices of the compounds are additionally formed by the C–Cl...π contacts for **I**–**III** and C–H...π contacts for **VI** (Table 4), and by hydrogen bonds: O–H...O in all compounds, C–H...O in **I**–**III** and **IV**, and C–H...Cl in **I**–**III** (Table 5).

Thus, we showed that the reaction of neodymium(III), samarium(III), europium(III), gadolinium(III), terbium(III), and dysprosium(III) nitrates with the sodium salt of dichlorophenoxyacetic acid (HL) in ethanol under identical conditions leads to crystallization of 1D polymers, the composition and structure of which is determined by the radius of the metal ion: [$LnL_3(C_2H_5OH)$] (Ln = Nd, Sm, Eu), [$LnL_3(H_2O)$] (Ln = Gd, Tb) and [$DyL_2(NO_3)$-$(C_2H_5OH)_2$]. It was demonstrated for the prepared

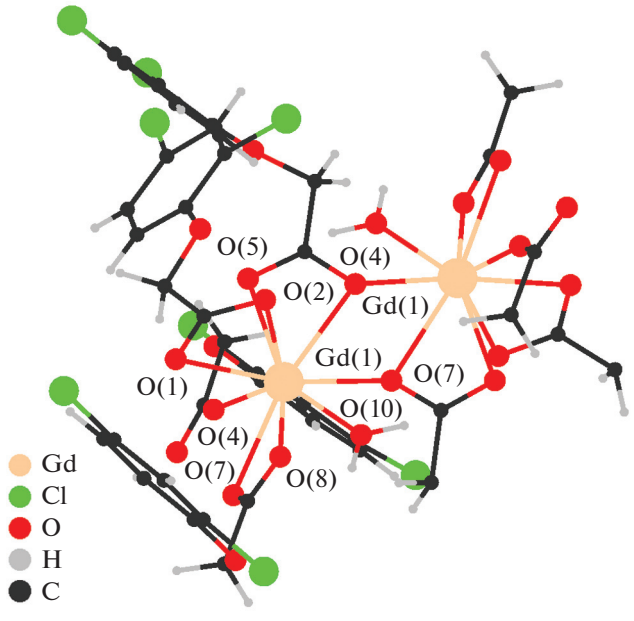

Fig. 2. Fragment of the polymer chain in **IV** (different coordination modes of the carboxylate anion are shown).

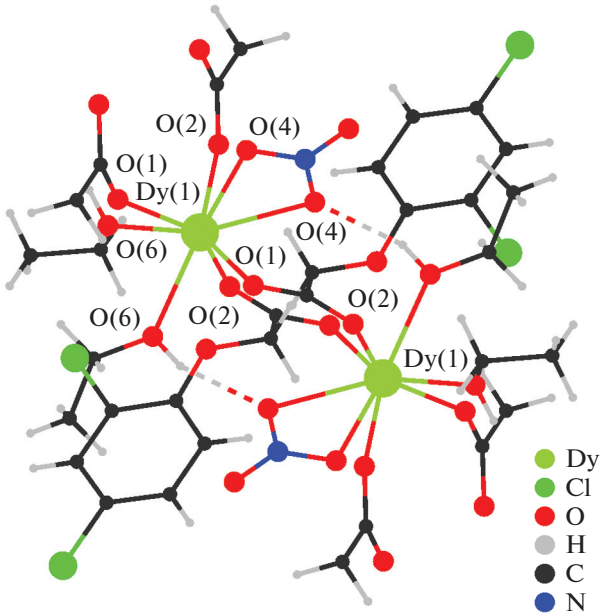

Fig. 3. Fragment of the polymer chain in **VI**.

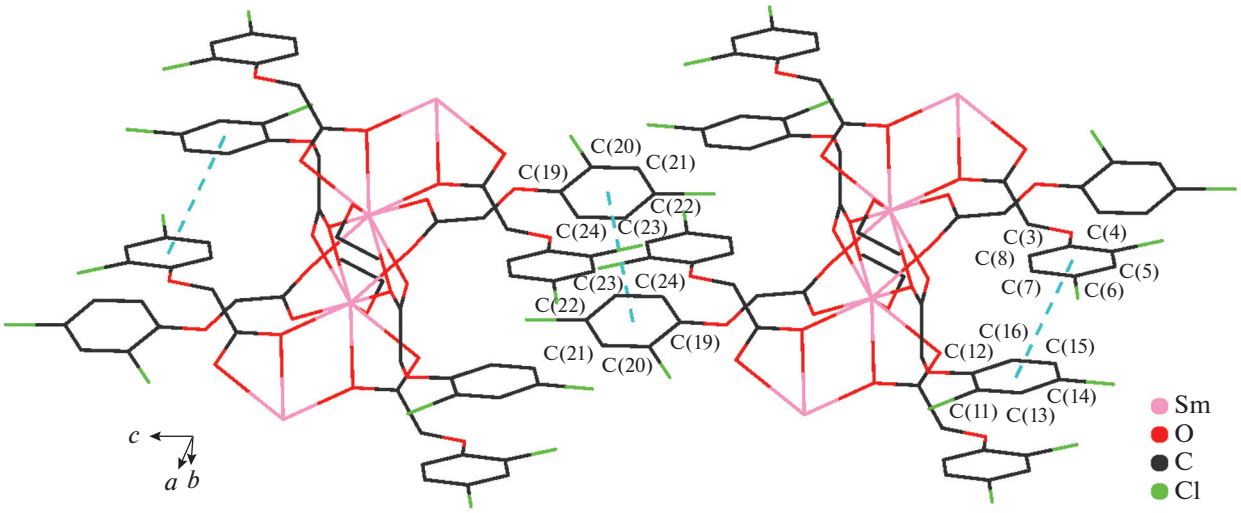

Fig. 4. Fragment of the crystal packing in **II** (the carbon atoms of the benzene rings connected by π...π interactions are numbered).

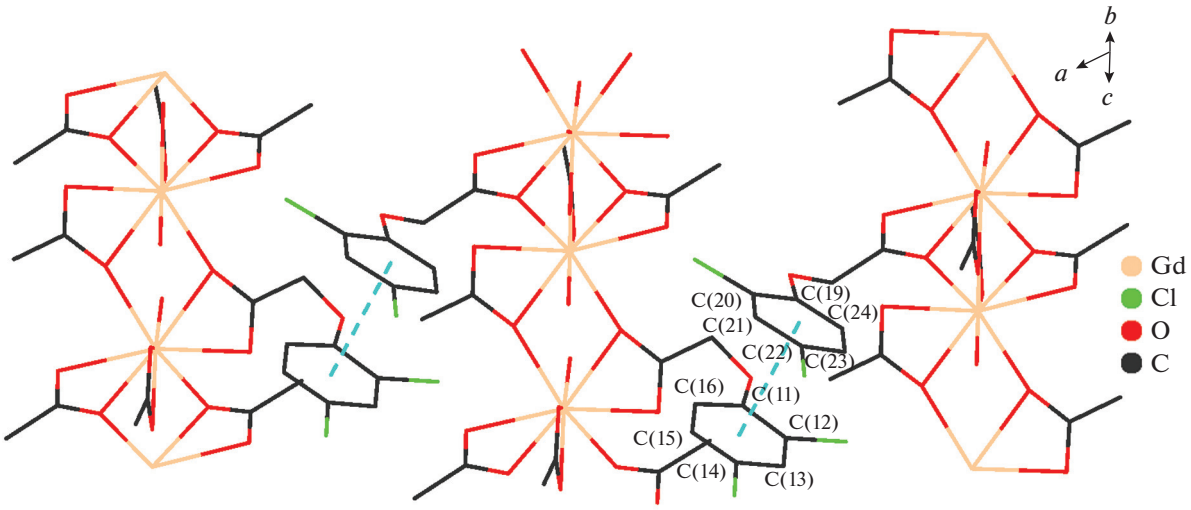

Fig. 5. Fragment of the crystal packing in **IV** (the carbon atoms of the benzene rings connected by π...π interactions are numbered).

series of compounds how the decrease in the metal ion radius in the series from neodymium(III) to dysprosium(III) determines the change in the coordination environment of the atom resulting from the competition of anions and neutral molecules. First, the two ethanol molecules in **I**–**III** are replaced by two smaller water molecules in **IV** and **V**, and on going to **IV**, ethanol molecules are again in the metal coordination sphere as a result of replacement of one carboxylate anion by a nitrate anion, which increases the steric accessibility of the coordination sites at the dysprosium atom.

ACKNOWLEDGEMENTS

The authors are grateful to the Center for Collective Use of Physical Investigation Methods of the Kurnakov Institute of General and Inorganic Chemistry, Russian Academy of Sciences, for the use of X-ray diffractometers.

FUNDING

The study was supported by the Ministry of Education and Science of Russia within the state assignment of the Kurnakov Institute of General and Inorganic Chemistry, Russian Academy of Sciences.

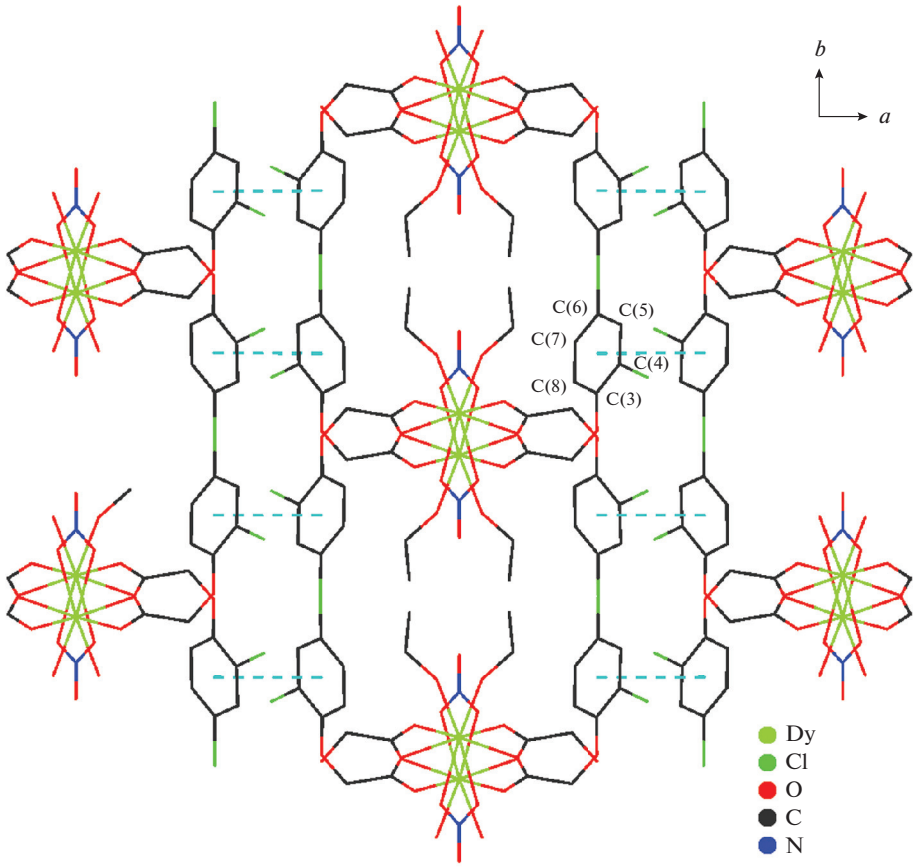

Fig. 6. Fragment of the crystal packing in **VI** (the carbon atoms of the benzene rings connected by π...π interactions are numbered).

Table 3. Parameters of π...π interactions in the crystal structures of **I**–**VI** (Cg_i is the benzene ring centroid; Cg–Perp is the shortest distance from Cg_i to the *j* plane of the neighboring ring, α is the angle between the Cg_i–Cg_j vector and the normal to *j* plane, Shift is the distance between the Cg_i and the perpendicular projection of Cg_j to the *i* plane)

Cg_i...Cg_j contact (symmetry code)	Cg_i···Cg_j, Å	Cg–Perp, Å	α, deg	Shift, Å
		I		
Cg(C(3)–C(8))...Cg(C(11)–C(16)) (1 – *x*, 1 – *y*, 1 – *z*)	3.893(5)	3.376(4)	3.5(4)	1.804
Cg(C(19)–C(24))...Cg((19)–C(24)) (1 – *x*, 1 – *y*, –*z*)	3.905(5)	3.621(4)	0	1.463
		II		
Cg(C(3)–C(8))...Cg(C(11)–C(16)) (1 – *x*, 1 – *y*, 1 – *z*)	3.874(5)	3.355(3)	3.7(4)	1.760
Cg(C(19)–C(24))...Cg((19)–C(24)) (1 – *x*, 1 – *y*, 2 – *z*)	3.899(5)	3.599(3)	0	1.499
		III		
Cg(C(3)–C(8))...Cg(C(11)–C(16)) (1 – *x*, 1 – *y*, 1 – *z*)	3.865(3)	3.347(2)	3.6(2)	1.766
Cg(C(19)–C(24))...Cg((19)–C(24)) (1 – *x*, 1 – *y*, 2 – *z*)	3.898(3)	3.600(2)	0	1.496
		IV		
Cg(C(11)–C(16))...Cg(C(19)–C(24)) (–1 + *x*, *y*, 1 + *z*)	3.631(9)	3.571(2)	8.0(3)	0.236
		VI		
Cg(C(3)–C(8))...Cg(C(3)–C(8)) (1/2 – *x*, 3/2 – *y*, 1 – *z*)	3.7152(16)	3.3628(11)	0.02(13)	1.579

Table 4. Parameters of Y–X···π interactions in the crystal packing of **I**–**VI** (Cg_i is the benzene ring centroid; X/Y···Cg is the distance from the centroid to the atom, X–Perp is the shortest distance from X atom to the ring plane, γ is the angle between the Cg_i–X vector and the normal to the *i* plane, Y–X···C*g* is angle)

Contact	X···Cg, Å	X–Perp, Å	γ, deg	Y–X···C*g*, deg	Y···C*g*, Å
			I		
C–C(l2)...Cg(C(11)–C(16)) (2 – *x*, 1 – *y*, 1 – *z*)	3.718(4)	3.479	20.67	77.6(3)	3.752(9)
C–C(l4)...Cg(C(3)–C(8)) (1 – *x*, 1 – *y*, 1 – *z*)	3.757(4)	3.338	25.59	68.3(3)	3.507(10)
C–C(l4)...Cg(C(19)–C(24)) (*x*, 1 + *y*, *z*)	3.543(4)	3.499	9.07	113.2(3)	4.523(11)
			II		
C–C(l2)...Cg(C(11)–C(16)) (–*x*, 1 – *y*, 1 – *z*)	3.728(4)	3.479	21.05	76.7(3)	3.736(10)
C–C(l4)...Cg(C(3)–C(8)) (1 – *x*, 1 – *y*, 1 – *z*)	3.765(4)	3.362	26.76	67.4(3)	3.489(10)
C–C(l4)...Cg(C(19)–C(24)) (*x*, –1 + *y*, *z*)	3.514(4)	3.470	9.05	113.7(3)	4.513(10)
			III		
C–C(l2)...Cg(C(11)–C(16)) (–*x*, 1 – *y*, 1 – *z*)	3.742(2)	3.486	21.28	76.09(17)	3.730(5)
C–C(l4)...Cg(C(3)–C(8)) (1 – *x*, 1 – *y*, 1 – *z*)	3.770(2)	3.364	26.84	67.23(17)	3.488(5)
C–C(l4)...Cg(C(19)–C(24)) (*x*, –1 + *y*, *z*)	3.515(2)	3.468	9.33	112.78(18)	4.489(5)
			IV		
C(9)–H...Cg(C(3)–C(8)) (1 – *x*, 1 – *y*, 1 – *z*)	2.68	2.67	6.30	147	3.556(3)

Table 5. Parameters of H-bonds in the crystals of **I**–**VI**

D–H...A contact	Distance, Å			D–H–A angle, deg
	D–Y	D...A	H...A	
		I		
O(10)–H(10)...O(8) (1 + *x*, *y*, *z*)	0.95	1.89	2.824(7)	166
C(2)–H(2B)...O(5) (1 – *x*, 1 – *y*, 1 – *z*)	0.99	2.49	3.356(9)	147
C(16)–H(16)...Cl(6) (1 – *x*, 1 – *y*, –*z*)	0.95	2.83	3.691(9)	152
C(18)–H(18A)...Cl(6) (1 – *x*, 1 – *y*, –*z*)	0.99	2.81	3.608(8)	138
C(25)–H(25B)...O(7)	0.99	2.59	3.260(10)	125
C(26)–H(26B)...O(5) (1 – *x*, 1 – *y*, 1 – *z*)	0.98	2.43	3.231(11)	139
		II		
O(10)–H(10)...O(8) (–1 + *x*, *y*, *z*)	0.95	1.90	2.845(7)	171
C(2)–H(2A)...O(5) (1 – *x*, 1 – *y*, 1 – *z*)	0.99	2.48	3.350(10)	146
C(16)–H(16)...Cl(6) (1 – *x*, 1 – *y*, 2 – *z*)	0.95	2.80	3.664(9)	152
C(18)–H(18B)...Cl(6) (1 – *x*, 1 – *y*, 2 – *z*)	0.99	2.80	3.599(8)	138
C(25)–H(25A)...O(7)	0.99	2.55	3.207(10)	124
C(26)–H(26B)...O(5) (1 – *x*, 1 – *y*, 1 – *z*)	0.98	2.40	3.203(11)	139
		III		
O(10)–H(10)...O(8) (–1 + *x*, *y*, *z*)	0.95	1.89	2.829(4)	169
C(2)–H(2A)...O(5) (1 – *x*, 1 – *y*, 1 – *z*)	0.99	2.46	3.327(5)	146
C(16)–H(16)...Cl(6) (1 – *x*, 1 – *y*, 2 – *z*)	0.95	2.81	3.660(5)	150
C(18)–H(18B)...Cl(6) (1 – *x*, 1 – *y*, 2 – *z*)	0.99	2.81	3.602(4)	137
C(25)–H(25A)...O(7)	0.99	2.56	3.207(6)	123
C(26)–H(26A)...O(5) (1 – *x*, 1 – *y*, 1 – *z*)	0.98	2.38	3.192(6)	139
		IV		
O(10)–H(10A)...O(2) (*x*, 1/2 – *y*, –1/2 + *z*)	0.89	1.95	2.705(8)	142
O(10)–H(10B)...O(1) (*x*, 1/2 – *y*, 1/2 + *z*)	0.89	2.40	3.180(9)	147
C(10)–H(10C)...O(5) (*x*, 1/2 – *y*, 1/2 + *z*)	0.97	2.59	3.001(8)	106
C(18)–H(18A)...O(8) (*x*, 1/2 – *y*, –1/2 + *z*)	0.97	2.57	3.050(9)	111
		VI		
O(6)–H(6)...O(4) (*x*, 1 – *y*, –1/2 + *z*)	0.84	2.04	2.844(3)	159

CONFLICT OF INTEREST

The authors of this work declare that they have no conflicts of interest.

REFERENCES

1. Hou, S.L., Dong, J., Tang, M.H., et al., *Anal. Chem.*, 2019, vol. 91, p. 5455.
2. Wen, G.X., Wu, Y.P., Dong, W.W., et al., *Inorg. Chem.*, 2016, vol. 55, p. 10114.
3. Yan, W., Wang, L., Yangxiao, K., et al., *Dalton Trans.*, 2016, vol. 45, p. 4518.
4. Wei, J.H., Yi, J.W., Han, M.L., et al., *Chem. Asian J.*, 2020, vol. 14, p. 3694.
5. Zeng, M.H., Yin, Z., Tan, Y.X., et al., *J. Am. Chem. Soc.*, 2014, vol. 136, p. 4680.
6. Zhou, L.J., Deng, W.H., Wang, Y.L., et al., *Inorg. Chem.*, 2016, vol. 55, p. 6271.
7. Kim, T.H., White, A.R., Sirdaarta, J.P., et al., *ACS Appl. Mater. Interfaces*, 2016, vol. 8, p. 33102.
8. Chen, D., Xu, W., Zhou, Y., et al., *J. Mater. Chem.*, 2017, vol. 5, p. 738.
9. Fan, Y., Guo, X., Zhang, Y., et al., *ACS Appl. Mater. Interfaces*, 2016, vol. 8, p. 31863.
10. Ji, W.-Q., Zhang, Q.-H., Wang, C.-F., et al., *Ind. Eng. Chem. Res.*, 2016, vol. 55, p. 11700.
11. Shang, M., Li, C., and Lin, J., *Chem. Soc. Rev.*, 2014, vol. 43, p. 1372.
12. Zhao, D., Rao, X., Yu, J., et al., *Inorg. Chem.*, 2015, vol. 54, p. 11193.
13. Andres, J., Hersch, R.D., Moser, J.-E., et al., *Adv. Funct. Mater.*, 2014, vol. 24, p. 5029.
14. De Bastiani, M., Saidaminov, M., Dursun, I., et al., *Chem. Mater.*, 2017, vol. 29, p. 3367.
15. Lin, J., Lai, M., Dou, L., et al., *Nat. Mater.*, 2018, vol. 17, p. 261.
16. Kang, X.M., Hu, H.S., Wu, Z.L., et al., *Angew. Chem., Int. Ed.*, 2019, vol. 58, p. 16610.
17. D'Andrade, B.W. and Forrest, S.R., *Adv. Mater.*, 2004, vol. 16, p. 1585.
18. Ouchi, A., Suzuki, Y., Ohki, Y., and Koizumi, Y., *Coord. Chem. Rev.*, 1988, vol. 92, p. 29.
19. Smith, G., Kennard, C.H.L., and White, A.H., *J. Chem. Soc., Perkin Trans.*, 1976, no. 7, p. 791.
20. Dendrinou-Samara, C., Drosou, D., Iordanidis, L., et al., *J. Inorg. Biochem.*, 2002, vol. 92, p. 156.
21. Guo, J., Liang, W.J., and Song, W.D., *Acta Crystallogr., Sect. E: Struct. Rep. Online*, 2007, vol. 63, p. 1595.
22. Shi, S.M., Chen, Z.F., and Liu, L., *J. Coord. Chem.*, 2008, vol. 61, p. 2725.
23. Ma, D., Qin, L., Zhao, H., et al., *Synth. Met.*, 2012, vol. 162, p. 2282.
24. Ma, D., Lu, K., Guo, H., et al., *J. Mol. Struct.*, 2012, vol. 1021, p. 179.
25. Gusev, A.N., Konnik, O.V., Shul'gin, V.F., et al., *Polyhedron*, 2023, p. 116749.
26. *SMART (control) and SAINT (integration) Sofware. Version 5.0*, Madison: Bruker AXS Inc., 1997.
27. Krause, L., Herbst-Irmer, R., and Stalke, D., *J. Appl. Crystallogr.*, 2015, vol. 48, p. 1907.
28. Sheldrick, G.M., *Acta Crystallogr., Sect. C: Struct. Chem.*, 2015, vol. 71, p. 3.
29. Dolomanov, O.V., Bourhis, L.J., Gildea, R.J., et al., *J. Appl. Crystallogr.*, 2015, vol. 42, p. 339.
30. Ruiz-Martínez, A., Casanova, D., and Alvarez, S., *Chem.-Eur. J.*, 2008, vol. 14, p. 1291.
31. Nakamoto, K., *Infrared and Raman Spectra of Inorganic and Coordination Compounds. Pt A: Theory and Applications in Inorganic Chemistry*, Hoboken: Wiley, 2009.

Translated by Z. Svitanko